

Feedback from quasars in star-forming galaxies and the triggering of massive galactic winds

Pierluigi Monaco & Fabio Fontanot

Dipartimento di Astronomia, Università di Trieste, via Tiepolo 11, 34131 Trieste, Italy - email: monaco, fontanot@ts.astro.it

Accepted ... Received ...

ABSTRACT

The shining of quasars is a likely trigger of massive galactic winds, able to remove most interstellar medium (ISM) from a star-forming spheroid. However, the mechanism responsible for the deposition of energy into the ISM is still unclear. Starting from a model for feedback in galaxy formation with a two-phase medium (Monaco 2004a), we propose that the perturbation induced by radiative heating from a quasar on the ISM triggers a critical change of feedback regime. In the feedback model, supernova remnants (SNRs) expanding in the hot and pressurized phase of a star-forming spheroid typically become pressure-confined before the hot interior gas is able to cool. In presence of runaway radiative heating by a quasar, a mass flow from the cold to the hot phase develops; whenever this evaporation flow is significant with respect to the star-formation rate, due to the increased density of the hot phase the SNRs reach the point where their interior gas cools before being confined, forming a thick cold shell. We show that in this case the consequent drop in pressure leads quickly to the percolation of all the shells and to the formation of a super-shell of cold gas that sweeps the whole galaxy. Radiation pressure is then very effective in removing such a shell from the galaxy. This self-limiting mechanism leads to a correlation between black hole and bulge masses for more massive bulges than $10^{10} M_{\odot}$.

The insertion of a motivated wind trigger criterion in a hierarchical galaxy formation model shows however that winds are not necessary to obtain a good black hole–bulge correlation. In absence of winds, good results are obtained if the mechanism responsible for the creation of a reservoir of low-angular momentum gas (able to accrete onto the black hole) deposits mass at a rate proportional to the star-formation rate. Using a novel galaxy formation model, we show under which conditions black hole masses are self-limited by the wind mechanism described above, and outline the possible observational consequences of this self-limitation.

Key words: galaxies: active - galaxies: bulges - intergalactic medium - quasars: general

1 INTRODUCTION

Active Galactic Nuclei (AGN) are intimately connected to the spheroidal components of galaxies. This is highlighted at low redshift by the correlation between the mass of the dormant black holes hosted in ellipticals and spiral bulges and their mass or central velocity dispersion (Kormendy & Richstone 1995; Magorrian et al. 1998; a more recent determination is given, e.g., by Marconi & Hunt 2003 or Häring & Rix 2004). The mass function of these black holes is found to be consistent with that inferred from the accretion history of quasars (Salucci et al. 1999; Yu & Tremaine 2002; Shankar et al. 2004; see also Haiman, Ciotti & Ostriker 2004). At higher redshift, quasars and radio galaxies are systemati-

cally found to be hosted at the centres of elliptical galaxies (see, e.g., Dunlop et al. 2003).

These pieces of evidence point to a connection between the formation of the two classes of objects. Many authors have proposed that feedback from the quasar could self-limit the bulge and black hole masses, forcing them to be proportional (see, e.g., Ciotti & Ostriker 1997; Silk & Rees 1998; Haehnelt, Natarajan & Rees 1998; Fabian 1999; Murray, Quataert & Thompson 2005). The dynamical importance of feedback is confirmed by N-body hydro simulations (see, e.g., Springel, Di Matteo & Hernquist 2004). Besides, elliptical galaxies, a homogeneous class of old, metal-rich, alpha-enhanced stellar populations with little ISM, have longly been supposed to form through a quick burst of star formation followed by a strong wind, able to wipe the galaxy out

of its ISM and to expel metals (especially iron) to the inter-cluster medium (ICM) (see, e.g., Renzini 2004). To reproduce the correlation between stellar mass and the level of alpha enhancement, this wind must halt star formation earlier in more massive galaxies (Matteucci 1994, 1996). Under this “monolithic” hypothesis, and using the shining of quasars as a clock for the formation of elliptical galaxies, Granato et al. (2001; 2004) succeeded in reproducing the main statistical properties of elliptical galaxies and quasars. Also the high level of chemical enrichment in quasars (see, e.g., Hamann & Ferland 1999) is well explained in this context (Matteucci & Padovani 1993; Romano et al. 2003).

On the other hand, many galaxy formation models based on hierarchical clustering are also successful in predicting the quasar–bulge connection, even in absence of an explicit self-limiting mechanism, by assuming simply that some fraction of cold bulge gas is accreted onto the black hole (Kauffmann & Haehnelt 2000; Cattaneo 2001; Cavaliere & Vittorini 2002; Hatziminaoglou et al. 2003; Mahmood, Devriendt & Silk 2004; Bromley, Somerville & Fabian 2004). However, the level of alpha-enhancement of stars in ellipticals is difficult to obtain in this framework (Thomas 1999).

The energy budget of an accreting black hole radiating with an efficiency $\eta = 0.1$ amounts to $\eta \dot{M}_\bullet c^2 \simeq 1.8 \times 10^{61} (M_\bullet / 10^8 M_\odot)$ erg. A $M_\bullet \simeq 1.6 \times 10^8 M_\odot$ black hole, which radiates 2.9×10^{61} erg during his life, is typically hosted by a $M_{\text{bul}} \simeq 10^{11} M_\odot$ bulge (see, e.g., Shankar et al. 2004). The binding energy of such a bulge (with velocity dispersion $\sigma \simeq 200 \text{ km s}^{-1}$) is of order $M_{\text{bul}} \sigma^2 \simeq 8.0 \times 10^{58} M_{\text{bul},11} \sigma_{200}^2$ erg (here $M_{\text{bul},11} = M_{\text{bul}} / 10^{11} M_\odot$ and $\sigma_{200} = \sigma / 200 \text{ km s}^{-1}$). It suffices then to inject ~ 0.3 per cent of the energy budget into the ISM of a forming galaxy to influence it strongly, e.g. to trigger a strong wind able to remove most ISM from the galaxy.

The mechanism responsible for this injection of energy is however unclear. In fact, a great part of the energy is emitted as UV-X radiation. Following Begelman (2004), a relatively hard UV-X source can affect the ISM by two main processes. The first is radiation pressure, exerted especially on dust grains, that can push matter in the radial direction. However, its efficiency in accelerating matter is of order v/c , where v is the bulk velocity of the gas in the radial direction. Its effectiveness in creating bulk motions of gas is then restricted to the neighbourhood of the central engine, where the r^{-2} dependence makes it very strong, thus compensating for the very low initial v/c . Recently, Murray et al. (2005) proposed that radiation pressure alone can drive a rather robust wind, able to remove some 10 per cent of the matter out of a bulge. This is true if the whole ISM is optically thick to radiation; we will come back to this point in Section 3.

Radiation pressure is also a good candidate for causing the strong outflows seen in Broad Absorption Line (BAL) quasars. These objects, relatively rare at the peak of quasar activity but rather common at high redshift (see, e.g., Maiolino et al. 2003), show outflows along the line of sight with velocity up to $\sim 0.1c$. The kinetic energy associated to these outflows is likely high; however, energy budget and effectiveness in triggering a galaxy-wide wind depend sensitively on the covering factor of the expelled gas. BAL quasars could correspond to a particular stage in which the quasar emits a very strong wind with a high covering factor; this stage should last much less than an Eddington time

($t_{\text{ed}} \simeq 4 \times 10^7 \text{ yr}$ for $\eta = 0.1$). Such an outflow would be effective in removing most ISM from the host galaxy (see, e.g., Granato et al. 2004). If instead BAL quasars correspond to rather common, low covering factor events, their ejection will most likely trigger star formation (similarly to what happens in radio galaxies, where radio jets are aligned with star-forming regions) more than quenching it by removing all the ISM.

Radiative heating is the second mechanism. Quasars emit UV-X light with a relatively hard spectrum, corresponding to inverse Compton temperatures of order $T_{\text{IC}} \simeq 2 \times 10^7 \text{ K}$ (see Sazonov, Ostriker & Sunyaev 2004b). Assuming thermal equilibrium in presence of this heating source, cold gas will be partially or totally heated to a temperature $\sim T_{\text{IC}}$ if radiation pressure is important with respect to the thermal one of the ISM (Krolik, McKee & Tarter 1981; Begelman, McKee & Shields 1983). Begelman (1985) estimated that such ablation could evacuate the inner region of Seyfert galaxies. Moreover, radiation pressure can accelerate cold clouds to some 100 km s^{-1} . In a typical star-forming spheroid, whose ISM is likely characterized by a high thermal pressure, radiative heating will perturb the ISM in the inner region of the galaxy, but taken alone it will not be able to cause a massive wind. Sazonov et al. (2004a) computed the effect of such heating on the ISM of a forming spheroid; in their calculation a wind is triggered when the fraction of old gas to total baryons is $\lesssim 1$ per cent, and star formation is almost over. As a result, the amount of ejected matter is modest.

The radiation pressure of a black hole accreting at a rate \dot{M}_\bullet at a distance r is (assuming an efficiency $\eta = 0.1$ as above and expressing the pressure in terms of P/k , where k is the Boltzmann constant):

$$\begin{aligned} \frac{P_{\text{rad}}}{k} &= \frac{L}{4\pi r^2 c k} \\ &\simeq 4.4 \times 10^7 \left(\frac{\dot{M}_\bullet}{4 M_\odot \text{ yr}^{-1}} \right) \left(\frac{r}{1 \text{ kpc}} \right)^{-2} \text{ K cm}^{-3}. \end{aligned} \quad (1)$$

This relation is calibrated on the Eddington accretion rate ($4 M_\odot \text{ yr}^{-1}$) of a $1.6 \times 10^8 M_\odot$ black hole hosted in a $10^{11} M_\odot$ bulge. For a star-forming spheroid the thermal pressure P_{th}/k can be as high as $10^5 - 10^6 \text{ K cm}^{-3}$ (see Section 2). The limit for the existence of a hot phase subject to runaway heating is $P_{\text{rad}}/P_{\text{th}} \gtrsim 7 - 27$ (Begelman et al. 1983). This is valid for plain inverse-Compton heating; heating by metal line absorption is very likely to contribute significantly (Ostriker & Ciotti 2004). Taking a condition $P_{\text{rad}} \geq 10 P_{\text{th}}$, runaway heating will be effective within a radius:

$$R_{\text{rh}} = 2.1 \left(\frac{\dot{M}_\bullet}{4 M_\odot \text{ yr}^{-1}} \right)^{1/2} \left(\frac{P_{\text{th}}/k}{10^6 \text{ K cm}^{-3}} \right)^{-1/2} \text{ kpc}. \quad (2)$$

This radius is of the same order of magnitude as the limiting radii reported by Sazonov et al. (2004a).

An element that has not been considered in the literature is that the perturbation induced by radiative heating will influence the way in which feedback from SNe works. In particular, radiation pressure can be very efficient in driving a massive wind if some other mechanism is able to generate a reasonably fast, optically thick outflow with a high covering factor. This can be provided by the percolation of many

SN remnants in the so-called Pressure-Driven Snowplough (PDS) phase, that takes place after part of the internal hot gas of the remnant has cooled and collapsed into a dense, cold shell (called “snowplough”, see, e.g., Ostriker & McKee 1988). In a previous paper (Monaco 2004a, hereafter paper I), we presented a model for feedback in galaxy formation. This model, which is described in Section 2, predicts that the ISM of a typical star-forming spheroid is characterized by a very hot and pressurized gas phase; this is able to halt the expansion of SN remnants much earlier than the time required by the internal gas to cool; the resulting SNRs are characterized by a very low porosity. We show in this paper that the insertion of a physically motivated evaporation term induced by the quasar leads very naturally (and without any tuning of the parameters) to a critical change of the feedback regime that causes, through the percolation of snowploughs, the creation of an optically thick super-shell that expands out of the galaxy at a speed of $\sim 200 \text{ km s}^{-1}$. Such a shell, pushed by radiation pressure, can be ejected out of a large spheroid, quenching star formation and leaving behind a hot rarified bubble. This mechanism can lead to a self-regulated black hole–bulge relation very similar to the observed one.

As mentioned above, the black hole–bulge relation can be generated simply by the mechanism responsible for the nearly complete loss of angular momentum, necessary to the gas to be able to accrete onto the black hole. A good fit is obtained if the accumulation of a reservoir of low-angular momentum gas proceeds at a rate proportional to the star formation rate in the bulge, or equivalently if a fraction of the cold bulge gas is systematically put into this reservoir. To assess the actual importance of winds in hierarchical galaxy formation, we insert a motivated wind criterion into a new galaxy formation model (that follow loosely the steps of commonly used “semi-analytic” models), and show with an example under which conditions the black hole mass is self-limited by winds more that determined by the reservoir mechanism.

The paper is organized as follows. Section 2 gives a very short summary of the model for feedback presented in paper I. Section 3 shows the effect of the introduction of a physically motivated evaporation term and discusses the triggering of the wind. In section 4 quasar-triggered winds are introduced in the galaxy formation model. Section 5 the conclusions. Preliminary results were shown by Monaco (2004c).

2 THE MODEL FOR FEEDBACK

We give here a brief description of the model for feedback presented in paper I; please refer to that paper for all details, and for a complete discussion of all the hypotheses.

Consider a volume V filled with a two-phase ISM, made up by a pervasive hot phase, of density and temperature n_h and T_h , and a distribution of cold clouds, of density and temperature n_c and T_c . Pressure equilibrium is assumed, so that $n_h T_h = n_c T_c$. Fixing the cold phase temperature to $T_c=100 \text{ K}$, it is very easy to express the filling factors of the two phases in terms of their temperatures and mass fraction (equation 2 of paper I).

Cold clouds are assumed to have a power-law mass function, $n(m_{cl})dm_{cl} \propto m_{cl}^{-\alpha_{cl}}dm_{cl}$. The parameter α_{cl} is set

here for simplicity to -2 , the expected value for a typical fractal distribution (Elmegreen 2002). The range of allowed masses is bounded below by a mass $m_l = 0.1 M_\odot$, and above by a mass m_u . The upper bound is fixed as follows: all clouds more massive than the Jeans mass m_J (that takes into account the non-sphericity of clouds, see Lombardi & Bertin 2001) collapse in a dynamical time t_{dyn} , form stars and are finally destroyed within another t_{dyn} . During the $\sim 2t_{dyn}$ period they acquire mass through unelastic collisions with smaller clouds, up to a mass m_u , computed with the aid of the Smoluchowski equation of kinetic aggregations. The fraction f_{coll} of cold gas involved in the star formation process is then equal to the fraction of mass in clouds with $m_J \leq m_{cl} \leq m_u$.

A fraction $f_* = 0.1$ of the collapsing cloud is transformed into stars. In Monaco (2004b) we showed that, due to the multi-phase nature of the ISM, the explosion of SNe leads to the destruction of the star-forming cloud in $\sim 3 \text{ Myr}$, leading to a modest loss of ~ 5 per cent of the energy budget. SN remnants percolate very soon, creating a single SB for each forming cloud. The SBs expand according to the solution of Weaver et al (1977); they propagate into the hot pervasive phase, their (modest) interaction with the cold clouds is neglected. The fate of SBs depends on the vertical scale-length of the system they belong to: if the system is thin enough, like in spiral discs, SBs blow out of the system before they are pressure-confined by the hot phase. In this case the efficiency of feedback in heating the local ISM (i.e. the fraction of energy given to the hot phase) is $f_E \sim 5 - 10$ per cent, while the remaining energy is injected into the external halo. For thicker systems, like a star-forming spheroid, SBs end by being confined by the pressure of the hot phase. Both blow-out and pressure confinement can take place either in the adiabatic expansion phase, where the thermal energy of the hot internal gas of the SB is conserved, or after that part of the internal gas has cooled down and collapsed to a cold shell, pushed by the pressure of the remaining hot gas (the PDS). When the PDS forms, the hot phase is not shock-heated any more but collapsed into the snowplough, so its net effect for the ISM is a loss of thermal energy.

Four different self-regulated feedback regimes can arise, depending on whether the SBs end by blow-out or pressure confinement, before or after the PDS stage starts. While blow-out in the PDS stage is not common, blow-out in the adiabatic stage is the typical feedback regime in galaxy discs. In a Milky Way-like case, the main properties of our local ISM are recovered. Adiabatic confinement is the typical regime found in thick system, while in very dense thick systems SBs are confined in the PDS regime. In some critical cases the hot phase is strongly depleted and the cold phase percolates the volume, giving thus rise to a burst of star formation.

In the following we concentrate on thick systems. In the adiabatic confinement regime, the details of the SB evolution are not important, as all the energy that manages to escape the star-forming cloud is given to the hot phase.

The system considered in paper I is composed by cold and hot gas phases, stars and an external halo (a passive reservoir of gas). Cold gas flows into the volume from the external halo on some specified infall time t_{inf} :

$$\dot{M}_{inf} = \frac{M_{halo}}{t_{inf}}. \quad (3)$$

Star formation proceeds at a rate:

$$\dot{M}_{\text{sf}} = f_{\star} f_{\text{coll}} \frac{M_{\text{cold}}}{t_{\text{dyn}}}, \quad (4)$$

and enriched gas is restored from dying stars (in an instantaneous recycling approximation) at a rate:

$$\dot{M}_{\text{rest}} = f_{\text{rest}} \dot{M}_{\text{sf}}, \quad (5)$$

where f_{rest} is the fraction of restored mass (assumed here to be 0.2). Besides, a fraction $f_{\text{evap}}=0.1$ of the star-forming cloud is evaporated by HII regions and SNe (see Monaco 2004b), giving origin to an evaporation flow:

$$\dot{M}_{\text{evap}} = f_{\text{evap}} f_{\text{coll}} \frac{M_{\text{cold}}}{t_{\text{dyn}}}. \quad (6)$$

The hot phase cools at a rate:

$$\dot{M}_{\text{cool}} = f_{\text{cool}} \frac{M_{\text{hot}}}{t_{\text{cool}}}, \quad (7)$$

where the cooling time t_{cool} is computed using the simple approximation proposed by Cioffi, McKee & Bertschinger (1988) and $f_{\text{cool}}=0.1$ is a parameter that regulates the passage from the hot to the cold phase (whose value depends on the complex density structure of the cooling gas). Finally, the hot phase typically is not confined within the star-forming region (the volume V that contains the ISM), so it leaks out at a rate:

$$\dot{M}_{\text{leak}} = \frac{M_{\text{hot}}}{t_{\text{leak}}}, \quad (8)$$

where the leaking time t_{leak} is the sound-crossing time of the structure.

The mass of the four components evolves according to this set of equations:

$$\begin{cases} \dot{M}_{\text{cold}} &= \dot{M}_{\text{inf}} + \dot{M}_{\text{cool}} - \dot{M}_{\text{sf}} - \dot{M}_{\text{evap}} \\ \dot{M}_{\text{hot}} &= -\dot{M}_{\text{cool}} - \dot{M}_{\text{leak}} + \dot{M}_{\text{evap}} + \dot{M}_{\text{rest}} \\ \dot{M}_{\star} &= \dot{M}_{\text{sf}} - \dot{M}_{\text{rest}} \\ \dot{M}_{\text{halo}} &= -\dot{M}_{\text{inf}} + \dot{M}_{\text{leak}} \end{cases} \quad (9)$$

An analogous system can be easily written for the metal flows.

The hot phase gains thermal energy from SNe (both through blasts and through the evaporated gas) at a rate:

$$\dot{E}_{\text{sn}} = E_{51} \frac{\dot{M}_{\text{sf}}}{M_{\star, \text{sn}}}, \quad (10)$$

where E_{51} is the energy of the single SN in units of 10^{51} erg (for simplicity we subtract from it any eventual loss due to the destruction of the star-forming cloud) and one SN progenitor is formed each $M_{\star, \text{sn}}$ of stars (we take $M_{\star, \text{sn}}=120 M_{\odot}$). Cooling and leak-out lead to energy losses at rates:

$$\dot{E}_{\text{cool}} = \frac{E_{\text{hot}}}{t_{\text{cool}}}, \quad (11)$$

$$\dot{E}_{\text{leak}} = \frac{E_{\text{hot}}}{t_{\text{leak}}}. \quad (12)$$

The evolution of the energy of the hot phase is then:

$$\dot{E}_{\text{hot}} = -\dot{E}_{\text{cool}} - \dot{E}_{\text{leak}} + \dot{E}_{\text{sn}}. \quad (13)$$

In case of PDS confinement, the \dot{E}_{sn} term must take into account the energy radiated away by the SB, while snowploughs generate a further mass flow \dot{M}_{snpl} from the hot

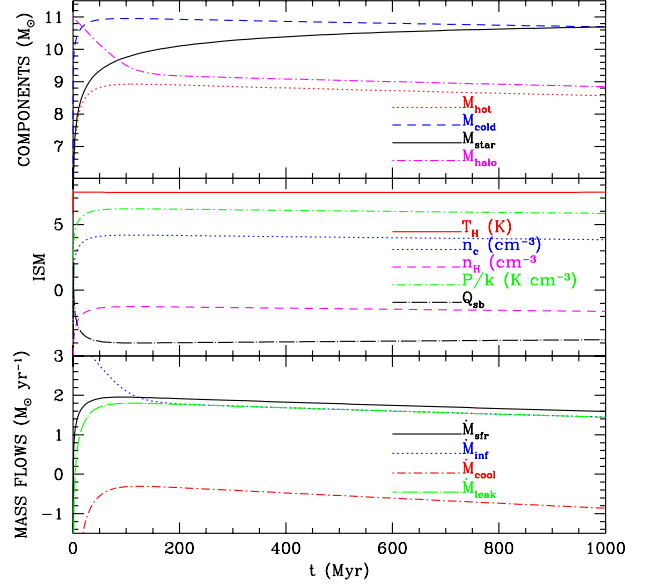


Figure 1. Evolution of a toy spheroid with the feedback model of paper I. $10^{11} M_{\odot}$ are first put into the external halo and then let infall on the “galaxy”. The upper panel shows the evolution of the mass in the four components (see the labels) as a function of time. The mid panel shows the evolution of the ISM (pressure, density of the two phases, temperature of the hot phase, porosity of SBs). The lower panel shows the main mass flows. All quantities in the y-axes are logarithmic.

to the cold phase, with the corresponding loss of thermal energy \dot{E}_{snpl} (see paper I for details).

As an illustrative example we show the evolution of a “monolithic” spheroid of mass $10^{11} M_{\odot}$ and half-mass radius (used as vertical scale-length) $R_{\text{hm}} = 4.9 \text{ kpc}$. Its circular velocity at R_{rhm} is 209 km s^{-1} , and its average density at the same radius is $0.1 M_{\odot} \text{ pc}^{-3}$. The infall time is assumed to be equal the dynamical time, $t_{\text{inf}}=2.5 \times 10^7 \text{ yr}$. Figure 1 shows the evolution of the four mass components, the main mass flows and the state of the ISM as a function of time. The cold gas accumulates quickly, but the efficient feedback prevents stars from forming as quickly. The ISM self-regulates to $P/k \sim 10^6 \text{ K cm}^{-3}$, $T_{\text{h}} \sim 2.5 \times 10^7 \text{ K}$, $n_{\text{h}} \sim 4 \times 10^{-2} \text{ cm}^{-3}$ and $n_{\text{c}} \sim 10^4$. Star formation regulates to a value of $\sim 50 M_{\odot} \text{ yr}^{-1}$, while infall and leak-out assume very similar values. Cooling is always negligible. Most importantly, the porosity Q_{sb} of the expanding SBs is always very low, as the blasts are very quickly halted by the high pressure of the external gas.

The feedback regime described above applies to the case when the cold gas infalls smoothly to the galaxy in small chunks, so that the creation of collapsing clouds is left to the coagulation mechanism introduced above. This is not the case in major mergers of disc galaxies; tidal disturbances in the last phases of the merger increase the thickness of the system, that switches then from adiabatic blow-out to adiabatic confinement. The sudden decrease of the Jeans mass, due to the increased pressure, adds then to the tidal disturbances in causing a diffuse burst of star formation on a dynamical timescale. However, only a fraction f_{\star} of each cloud is transformed into stars, so this burst will contribute

to the increase of pressure but will not consume a very large amount of stars. Tidal disturbances, besides helping the triggering of star formation in clouds, will also stretch and fragment them in small pieces, helping the system to get into the new regime. Most gas will then be transformed into stars when the new feedback regime has taken place.

A more thorough description of this process and a more careful comparison to observations is left to a forthcoming paper. Here we notice only that the adiabatic confinement regime implies the presence of significant amounts of molecular gas (with such a high n_c molecular hydrogen should be present even in non-collapsing clouds) in conjunction with a relatively modest star formation activity. This is nicely consistent with the observation of cold gas in elliptical galaxies at the centre of massive cooling-flow clusters (see, e.g., Edge & Frayer 2003).

3 FEEDBACK FROM THE QUASAR

3.1 The effect of radiative heating

We assume for the moment that the whole galaxy is affected by radiative heating in the same way. To model the perturbation induced by this heating we add to the system described above a seed black hole of $1000 M_\odot$, accreting mass at the Eddington rate for the whole period. We model radiative heating as an evaporation term \dot{M}_{rh} , proportional to the accretion rate onto the black hole \dot{M}_\bullet , that moves mass from the cold to the hot phase:

$$\dot{M}_{\text{rh}} = k_{\text{rh}} \dot{M}_\bullet. \quad (14)$$

This term gives a positive contribution to the \dot{M}_{hot} equation and a negative one to the \dot{M}_{cold} equation in the system 9. The corresponding energy flow term, \dot{E}_{rh} , is obtained assuming that the gas is heated to the inverse Compton temperature of the AGN, $T_{\text{IC}} = 2 \times 10^7$ K:

$$\dot{E}_{\text{rh}} = \frac{3}{2} k T_{\text{IC}} \frac{\dot{M}_{\text{rh}}}{\mu m_p} \quad (15)$$

(here μ is the mean molecular weight of the hot phase, and is self-consistently computed in the model). The global heating rate of the quasar is $6.7 \times 10^{44} \tau T_{\text{IC}8} L_{46}$ erg s^{-1} (Begelman 1985), where τ is the electron scattering optical depth of the cold phase, $T_{\text{IC}8} = T_{\text{IC}}/10^8$ K and L_{46} is the ionizing radiation of a quasar in units of 10^{46} erg. The optical depth can be written as that of a single cloud, τ_{cl} , times the covering factor \mathcal{C} of the cold phase. For a typical AGN spectrum a fraction $f_{\text{ion}} \simeq 37$ per cent of the radiated energy is above the Lyman limit¹. In this case $L_{\text{ion}} = 2.0 \times 10^{45} \dot{M}_\bullet$ erg s^{-1} , where \dot{M}_\bullet is in units of $M_\odot \text{yr}^{-1}$. The constant k_{rh} of equation 14 is then estimated by equating the heating rate to the thermal energy gained by the evaporated mass. We obtain:

$$k_{\text{rh}} = 104 \tau_{\text{cl}} \mathcal{C}. \quad (16)$$

¹ This is computed using the quasar template spectrum of Cristiani & Vio (1990) down to 538 \AA , extrapolated to 300 \AA with the recipe of Risaliti & Elvis (2004). At shorter wavelength (between 0.01 and 30 \AA) we use a power-law with a photon index of $\Gamma = -1.8$ (see Comastri et al., 1995). The relative normalization is fixed by assuming $\alpha_{\text{ox}} = -1.63$ (Vignali et al. 2003). The interpolation between 30 and 300 \AA follows Kriss et al. (1999).

This is likely to be a lower limit, due to the neglected metal line heating. The cold phase of a highly pressurized ISM like that of Figure 1, with the mass subdivided into many small clouds, presents a rather high covering factor², $\mathcal{C} \sim 0.3$. The value of τ_{cl} could be low for these very high density clouds. However, in a more realistic setting a significant fraction of the cold phase would be in a warm intermediate phase, with $T \sim 10^4$. While a modeling of the dynamical role of this warm phase is beyond the interest of this paper, it is clear that this phase would present significant values of τ_{cl} and \mathcal{C} . Heating by metal lines would obviously strengthen this conclusion. On the other hand, attenuation by diffuse dust would give lower evaporation rates. As a conclusion, we reckon that a value of ~ 20 - 50 for k_{rh} is reasonable. Begelman (1985, 2004) quotes an evaporation rate of $20 - 200 \mathcal{C} (L_{\text{ion}}/10^{46} \text{ erg}) M_\odot \text{yr}^{-1}$ for a spiral-like ISM. This would correspond to $k_{\text{rh}} = 4 - 40 \mathcal{C}$, lower than the value quoted above. But Begelman's calculation refers to the rather different case of a wind generated in a spiral galaxy by a central AGN. In our case the geometry of the system is rather different, and we do not require that the gas is ejected out of the galaxy in a wind. This justifies the higher evaporation rate.

Figure 2 shows the effect of this heating term on the system. As soon as the radiative heating mass flow becomes comparable to the other ones (\dot{M}_{sf} , \dot{M}_{eak} and \dot{M}_{inf}), ~ 400 Myr after the beginning, the density of the hot phase starts increasing. The pressure grows, while the temperature of the hot phase starts to decrease, due to the enhanced cooling. SBs are confined by the enhanced pressure earlier and earlier, and Q_{sb} decreases considerably. When n_h grows large enough, the system switches to the PDS confinement feedback regime. In this case a significant amount of energy from SNe is radiated away before the blast is pressure-confined by the hot phase. The resulting snowploughs move mass from the hot to the cold phase, causing a sudden decrease of the density and temperature of the hot phase. This leads to a drop in thermal pressure, with a consequent increase of the Jeans mass of cold clouds and of the star formation rate.

Most importantly, just after the change to the PDS confinement regime has taken place, the porosity of the SBs jumps suddenly from very low to > 1 values. This means that the SBs percolate into a unique super-SB, a cold super-shell that sweeps the galaxy, cleaning it very efficiently from all of its ISM. The final velocity of SBs at the formation time of the super-shell will not be much higher than the thermal velocity of the hot phase, $\sim 200 \text{ km s}^{-1}$. This means that the outgoing mass will be accelerated by radiation pressure with an initial efficiency of ~ 0.06 per cent. This efficiency will grow as the shell is accelerated to a higher speed.

The percolation of a diffuse distribution of blasts will produce not only an outgoing supersonic super-shell. A significant fraction of the mass will be compressed to the centre of the galaxy by the same blasts. This is well illustrated, for instance, by the simulation of Mori, Ferrara & Madau (2002)

² We have $\mathcal{C} = 3 f_c R / 4 a_{\text{cl}}$, where f_c is the filling factor of the cold phase, R the size of the structure and a_{cl} the typical size of the cold clouds. For the model in Figure 1, $f_c \sim 2 \times 10^{-4}$ and $a_{\text{cl}} \sim 1 \text{ pc}$, so that for $R \sim 2 \text{ kpc}$ (the size at which a typical $10^{11} M_\odot$ bulge with an Eddington-accreting black hole is heated) $\mathcal{C} \sim 0.3$.

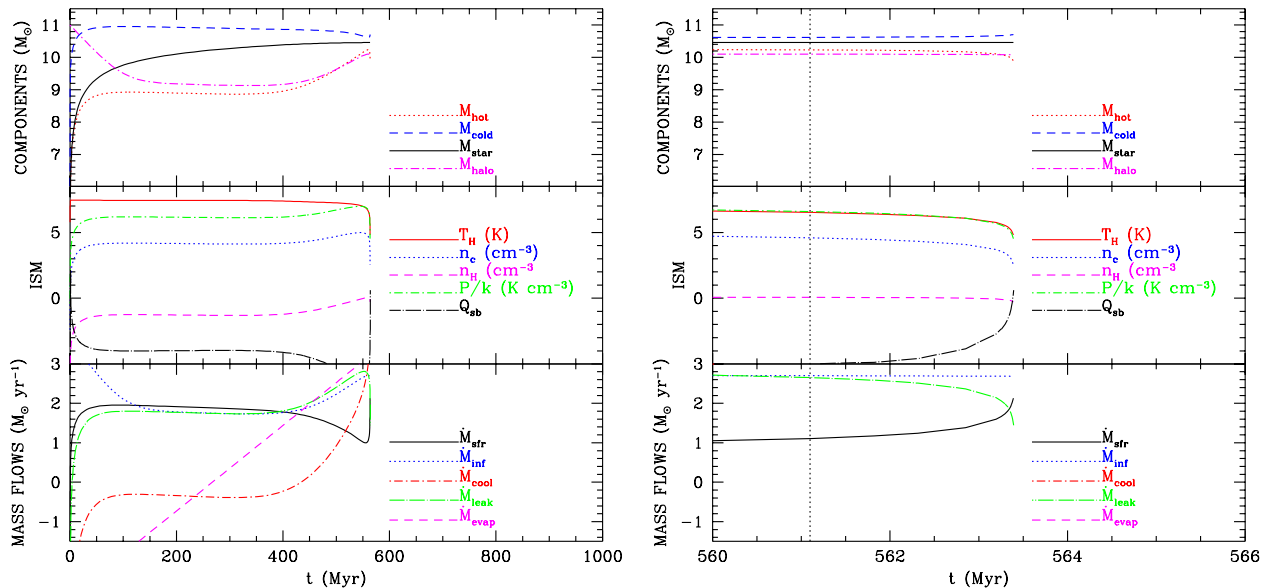


Figure 2. As in Figure 1 for the evolution of the toy spheroid in case of runaway radiative heating. The right panel shows a detail of the critical change of regime; the dotted vertical line denotes the starting time of the PDS confinement regime.

of a blow-out in a primordial galaxy. Though the physical scales and the energetic budget involved are quite different, the geometry and the astrophysics of the problem are similar. In their simulations a fraction of order of 10 per cent of the gas (the precise number depending on the distribution of the star-forming clouds) is compressed to the centre of the halo, while the rest is blown away. In our case, the gas compressed to the centre will give rise to a secondary burst of star formation and to further accretion onto the black hole. This will eventually give more energy to the super-shell, both in terms of new SNe giving thermal energy to the rarified hot gas and in terms of new radiation pressure from the accreting black hole. Moreover, if the ISM is dusty in the starburst phase, the dust will be destroyed by the quasar or removed by the wind just after the percolation phase. The main unobscured shining phase of the quasar could then correspond to the accretion of the matter compressed to the centre by the blasts.

The super-shell will form mainly by the sweeping of the hot phase, which at the onset of PDS confinement amounts to ~ 20 per cent of the mass, while the very dense cold clouds (~ 50 per cent of the mass) will be affected less strongly. So, the super-shell may leave some cold mass behind. However, it is likely that this mass will be promptly consumed into stars, for the following reasons. Radiative heating acts preferentially on cold clouds, so the matter left will be in relatively large clouds, where star formation is easier to trigger. At the super-shell formation, sweeping by the supersonic shells will trigger star formation in many of the remaining clouds. After the formation of the super-shell, the galaxy will be filled with hot, pressurized gas, able to thermo-evaporate the leftovers of the star formation process (which amount to ~ 90 per cent of the mass involved in star formation). Moreover, radiative heating and radiation pressure themselves can pressurize the clouds, stimulating star formation (Begelman 1985). As a conclusion, it is likely that the cold

gas left behind by the shell will be promptly consumed into stars or evaporated.

From this toy model we learn that the galactic wind is triggered whenever the evaporation rate is roughly a factor of 10 larger than the (unperturbed) star formation rate. As this quantity scales with the initial gas mass, and as the Eddington accretion rate is proportional to the black hole mass, this “monolithic” toy model implies a correlation between stellar and black hole masses, due to the self-limiting feedback from the quasar. However, the black hole mass at the shining time is $\sim 2 \times 10^9 M_\odot$, much larger than what expected in this spheroid. Moreover, no mention is done here on how gas manages to lose angular momentum so as to be able to accrete onto the black hole.

3.2 Radiation pressure on the expanding super-shell

The mass that can be accumulated initially in the super-shell is limited by the kinetic energy that the shell can receive from SNe. Figure 2 shows that at the percolation time the star formation is as high as $\sim 100 M_\odot \text{ yr}^{-1}$. For $M_{*,\text{SN}}=120 M_\odot$, this corresponds to 0.83 SN per year. This level of star formation will be sustained for at least one shell-crossing time, which is the time required to the shell to form. For a fiducial initial velocity $v_i = 200 \text{ km s}^{-1}$, coincidentally very similar to the circular velocity of a $10^{11} M_\odot$ bulge at the half-mass radius ($R_{\text{hm}} = 4.9 \text{ kpc}$), $V_c = 209 \text{ km s}^{-1}$, the shell crossing time is very similar to the dynamical time of the bulge, $2.5 \times 10^7 \text{ yr}$, and also to the time required to an $8-M_\odot$ star to explode. In this time about 2.2×10^7 SN progenitors are formed, for an energy budget of $\sim 2 \times 10^{58}$ erg. The kinetic energy of a $10^{10} M_\odot$ shell (amounting to 10 per cent of the total mass) traveling at 200 km s^{-1} is $\sim 4 \times 10^{57}$; it will be accelerated by SNe if a reasonable 20 per

cent efficiency is assumed. However, this is likely to be only a lower limit. Indeed, such a starburst consumes only $2.5 \times 10^9 M_\odot$ of stars. In other words, $\sim 4 M_\odot$ are accelerated for each M_\odot of stars formed. As commented above, the formation of the supershell will likely trigger a burst of star formation, both by compressing cold gas to the centre and by sweeping the most massive cold clouds. If for instance $10^{10} M_\odot$ of gas are transformed into stars during the formation of the supershell, the fraction of mass that can be accelerated by SNe raises to 40 per cent. We conclude that the available energy from SNe does not put strong constraints on the amount of mass that can be accelerated.

The amount of mass that can be ejected in a wind is instead limited by the ability of radiation pressure to perform work on the shell. Due to its high pressure, the gas in the shell is not subject to runaway radiative heating until it becomes subsonic or is destroyed by Raileigh-Taylor instabilities. While sweeping the hot gas phase and, later, the hot halo gas pervading the dark matter halo that surrounds the galaxy, the super-shell grows in mass. It is slowed down by gravity, pressure from the external hot gas and mass load.

The equation of motion of a super-shell of mass M_s , radius R_s and velocity v_s can be written as follows:

$$\frac{1}{2} M_s \frac{dv_s^2}{dR_s} = -v_s^2 \frac{dM_s}{dR_s} - GM_s \frac{M_{\text{tot}}(R_s)}{R_s^2} + (P_{\text{rad}} + P_{\text{int}} - P_{\text{ext}}) 4\pi R_s^2. \quad (17)$$

We will neglect the internal pressure term, P_{int} , and concentrate on radiation pressure (equation 1).

Let's first assume that a shell of constant mass is leaving an isolated bulge of mass M_{bul} ; no dark matter component is considered at the moment. Fitting the data of Marconi & Hunt (2003), we find that the half-mass radius ($R_{\text{hm}} = 1.35R_e$, where R_e is the effective radius) of an elliptical galaxy scales with the bulge mass as follows:

$$R_{\text{hm}} = 4.9 M_{\text{bul},11}^{0.65} \text{ kpc}. \quad (18)$$

The scatter around this relation is ~ 0.3 dex. For the mass profile we assume for simplicity a roughly constant rotation curve, so that $M_{\text{bul}}(r) \propto r$. We then fix the value of $M_{\text{bul}}(r)/r$ to its value at the half-mass radius, $M_{\text{bul}}/2R_{\text{hm}}$.

The mechanical pressure exerted by radiation depends on the optical depth of the shell, $P_{\text{rad}}(1 - e^{-\tau_{\text{shell}}})$. The column density of a shell of mass $M_s = f_s M_{\text{bul}}$ at a radius R (in kpc) is $8.0 \times 10^{23} f_s M_{\text{bul},11} R^{-2} \text{ cm}^{-2}$. Following Begelman (2004), electron scattering gives only $\tau_{\text{shell}} \sim 0.7x f_s M_{\text{bul},11} R^{-2}$, where x is the ionization fraction. Photoionization gives $\tau_{\text{shell}} \sim 100 (P_{\text{th}}/P_{\text{rad}}) f_s M_{\text{bul},11} R^{-2}$. As long as the shell propagates supersonically, its pressure is very high, so the value of τ_{shell} at $P_{\text{th}} = P_{\text{rad}}$ is a very conservative lower bound. The high pressure guarantees also that the shell is not affected by runaway radiative heating. Dust absorption on the other hand gives $\tau_{\text{shell}} \sim 10^5 f_s M_{\text{bul},11} R^{-2}$. Moreover, the ratio between the mean free path of the dust grains and the thickness of the shell results $\sim 4 \times 10^{-5} f_s^{-1} M_{\text{bul},11}^{-1} R^2$ (Murray et al. 2005), so that dust grains are hydrodynamically coupled to the fluid. As a conclusion, the shell absorbs most of the quasar light from ~ 4000 to $\sim 1 \text{ \AA}$, so that radiation pressure (equation 1) can be safely used in equation 17. This is valid until the shell

is so diluted that $\tau_{\text{shell}} \sim 1$, which happens only at several half-mass radii.

Solving equation 17, we find that the kinetic energy of the shell, K_s , evolves like:

$$K_s = -f_s M_{\text{bul}} V_c^2 \ln \left(\frac{R_s}{R_i} \right) + \frac{L}{c} (R_s - R_i) + K_i. \quad (19)$$

Here V_c is the circular velocity of the bulge at R_{hm} , and the suffix i refers to the initial conditions, so that $K_i = f_s M_{\text{bul}} v_i^2/2$. Requiring that the minimum of K_s is positive, we obtain an upper limit on f_s which is given by the largest root of the algebraic equation $(a + \ln(b/f_s))f_s - b = 0$, where $a = 1 + v_i^2 R_{\text{hm}}/GM_{\text{bul}}$ and $b = 2R_{\text{hm}}LR_i/GM_{\text{bul}}^2 c$. Scaling the accretion rate to $4 M_\odot \text{ yr}^{-1}$ (the Eddington accretion rate of a $1.6 \times 10^8 M_\odot$ black hole hosted in a $10^{11} M_\odot$ bulge) and assuming that the initial radius of the shell is that at which radiation pressure equals the thermal one (equation 2), we obtain that the upper limit to f_s is fit (within ~ 15 per cent) by the following formula:

$$f_s < 0.21 \left(\frac{\dot{M}_{\bullet,4}}{M_{\text{bul},11}^{1.1}} \right)^{1.5}. \quad (20)$$

(here $\dot{M}_{\bullet,4} = \dot{M}_\bullet/4 M_\odot \text{ yr}^{-1}$).

Radiation pressure is then able to expel up to 21 per cent of the mass of a star-forming spheroid if its black hole follows the known black hole–bulge relation and is accreting at the Eddington ratio. More active black holes can remove much larger amounts of mass (assuming that star formation is strong enough to create such massive super-shells). This provides a self-limiting mechanism able to generate a black hole–bulge correlation very similar to that observed³.

This result is valid for bulges with escape velocities larger than 200 km s^{-1} . Less massive bulges than $10^{10} M_\odot$ have escape velocities below this limit, so mass removal is efficient even in case of no accretion. This implies a much looser black hole–bulge correlation at such masses.

Once the super-shell has left the galaxy, it interacts with the hot gas pervading the dark matter halo. In this case the gravity term of equation 17 contains also the contribution of the halo, while the hot halo gas slows down the shell by mass load and thermal pressure. We have verified that for reasonable values of the halo parameters (mass, concentration, gas distribution etc.) the shell will be promptly stopped as soon as it interacts with the gas. At this point it will fragment. At a speed of $\sim 200 \text{ km s}^{-1}$, a distance of a few tens of kpc is reached in several tens of Myr, i.e. ~ 2 -3 Eddington times. If the accretion of the material compressed at the centre started promptly at shell formation, and if the quasar were visible only after the shell is destroyed, then most accretion would be hidden by the dusty shell. However, the time necessary to the gas compressed to the centre to lose its angular momentum is likely to be not negligible. For instance, Granato et al. (2004) suggest a timescale for viscous accretion of order $5 \times 10^7 \text{ yr}$ for a black hole of $10^8 M_\odot$ in a 200 km s^{-1} bulge, amounting to ~ 1.2 Eddington times. We suggest as a likely scenario that while the shell is pushed

³ Equation 2 is used assuming a constant gas pressure for all bulges. Smaller bulges are however denser. From the model described in Section 2 we find that roughly $P_{\text{th}} \propto M_{\text{bul}}^{-0.5}$. Taking this into account, we obtain $f_s \lesssim 0.2 (\dot{M}_{\bullet,4}/M_{\text{bul},11}^{0.9})^{1.5}$.

by accretion of the low-angular momentum gas accumulated during the stage of self-limited star formation (in the adiabatic confinement feedback regime), the accretion of the material compressed at the centre at the super-shell formation takes place mostly after the shell has been destroyed.

The drop in pressure consequent to the shell destruction makes radiative heating effective again and, due to the very high covering factor of the shell gas, a part of it can be in principle heated back to T_{IC} . However, it is easy to verify that the heating time evolves like $t_{\text{heat}} \sim 1.2 \times 10^8 R^2 L_{46}^{-1} (T/T_{\text{IC}}) N_{H,24}$ yr, where T is the temperature of the heated gas and $N_{H,24}$ the column density of the layer that is affected by heating, in units of 10^{24} cm^{-2} (see Begelman 2004). Clearly, for distances significantly larger than one kpc, the heating time becomes too large for run-away heating to be effective. In this case the shell will be heated to a much lower temperature than T_{IC} .

During the expansion, radiation pressure performs a work LR_s/c on the super-shell. For $\dot{M}_\bullet = 4 M_\odot/\text{yr}$ and $L = 2.3 \times 10^{46}$, at a fiducial distance of 20 kpc (roughly 5 half mass radii, at which the effects of the dark-matter and hot-gas halo should be important) the AGN has given 4.7×10^{58} erg to the shell. The efficiency of energy injection depends on the actual expansion velocity, which however does not exceed much the initial one if the shell is near its mass limit. Besides, for $k_{\text{rh}} = 50$ and $\dot{M}_\bullet = 1.6 \times 10^8 M_\odot$, radiative heating injects 6.5×10^{59} erg into the ISM, amounting to 2 per cent of the energy budget. However, most of this energy is lost to radiation during the formation of the super-shell. This calculation confirms that the energetic efficiency of feedback from quasars is very likely smaller than 1 per cent. In this case, the 5 per cent efficiency used in the simulations of Springel et al. (2004) seems a rather extreme choice.

To understand the robustness of these conclusions, we have repeated the computation of the fraction of mass removed by the wind under several different assumptions on the mass profile, obtaining in most cases a fraction of order of 10 per cent times $(\dot{M}_{\bullet,4}/M_{\text{bul},11})$ to the power 1.5–2 ($M_{\text{bul},11}$ may be raised to a power very similar to one).

As a conclusion, radiation pressure can remove about 20 per cent of the mass of a star-forming spheroid hosting an Eddington accreting black hole that follows the local black hole–bulge relation. However, it cannot remove this gas from the massive dark-matter halo that hosts the bulge.

3.3 Feedback from AGN in presence of other stellar feedback regimes

The mechanism described above depends on the assumption that feedback is in the adiabatic confinement regime when the quasar shines. Here we show that the validity of the numbers given above is more general.

As shown in Monaco (2004b), small star-forming clouds are destroyed by a single SN. As the number of SNe per cloud is rather small, the fraction of energy lost in destroying the cloud could be rather high. This justifies a lower effective value for E_{51} in the case of adiabatic confinement. In paper I it was found that, for $E_{51}=0.3$, the system goes to the PDS confinement regime. This has the effect of lowering the pressure and increasing the porosity. The onset of the PDS confinement regime can be smooth (as the example given in

paper I) or critical; for the infall times used here the onset is critical, leading to the percolation of SBs. This will lead to critical, self-stimulated bursts of star formation, that will increase the pressure and make the solution bounce back to the adiabatic confinement one. In principle, this would lead to the creation of a galaxy-wide super-shell. However, in absence of a synchronized trigger as a shining quasar, this explosion will presumably interest different parts of the galaxy at different times; moreover, even in case a super-shell is formed, its velocity will be lower than the escape velocity of the cloud, so the cold gas will fall back soon if $M_{\text{bul}} > 10^{10} M_\odot$. As a conclusion, the system will spend most of its time in the adiabatic confinement regime, with possible (self-stimulated and quickly self-quenched) bursts of star formation; consequently, the effect of radiative heating will be similar to what described above.

Murray et al. (2005) estimated that radiation pressure by an Eddington accreting black hole can wipe out some 10 per cent of the mass of an optically thick spheroid simply by radiation pressure. Also this self-limiting mechanism induces a black-hole bulge relation compatible with observations. Repeating their calculation for our $10^{11} M_\odot$ case spheroid we obtain $f_s < 0.06\mathcal{C}$. Clearly, the presence of an outward-moving shell with $\mathcal{C} = 1$ makes the case for a massive wind driven by radiation pressure much more convincing.

4 SHINING QUASARS IN THE HIERARCHICAL CONTEXT

All the calculations given above assume that an Eddington-accreting black hole is present in a star-forming spheroid, and do not take into proper account two very important aspects of galaxy and quasar formation, namely the formation and evolution of galaxies driven by the hierarchical assembly of dark matter halos, and the nearly complete loss of angular momentum necessary to the gas to accrete onto the central black hole. We show in the following how the results of Section 3 apply when inserted into a hierarchical galaxy formation model, with simple assumptions on the loss of angular momentum.

To show in which conditions quasar-triggered winds will lead to a self-limited black hole–bulge relation, we present an example obtained by inserting reasonable rules for quasar accretion into a hierarchical galaxy formation model. This model is still under construction, and will be presented in full detail elsewhere. The aim here is not to present a proper complete modeling of galaxies and quasars, but just to illustrate how the triggering of galaxy winds may behave in a more realistic situation than a “monolithic” spheroid.

4.1 The galaxy formation model

The model follows loosely the “semi-analytic” models of Kauffmann et al. (2000), Cole et al. (2000), Somerville, Primack & Faber (2000), Menci et al. (2002), Hatton et al. (2003), Kang et al. (2004). Here we give a very quick description of the ingredients used.

(i) Merger histories of dark matter halos are obtained with the PINOCCHIO tool (Monaco et al. 2002; Monaco, Theuns & Taffoni 2002; Taffoni, Monaco & Theuns 2002). (ii)

The survival and merger of substructure (galaxies) is modeled using the results of Taffoni et al. (2003). (iii) Gas in the dark matter halos is shock-heated, and is assumed to be in hydrostatic equilibrium. It is treated as a polytropic gas with polytropic index 1.1 – 1.3. (iv) Radiative cooling is described with the cooling function of Sutherland & Dopita (1993). The evolution of the cooling radius is followed taking into account also the hot gas emitted by star-forming galaxies. (v) The cooled gas is put into a cold halo gas component, that is then let infall on the central galaxy in a few infall timescales. (vi) Whenever the hot halo gas is hotter than the virial temperature, it is ejected to the external space as a wind. It is then acquired back again by the halo when its virial temperature is equal to the temperature of the gas at the escape time. (vii) The same thing happens to the cold gas whenever its kinetic energy overtakes the virial value. (viii) The disc structure is computed with the Mo, Mao & White (1998) model, taking into account the presence of a bulge. (ix) Star formation and feedback in discs are computed with the aid of an extended Schmidt law, based on the results of paper I. Feedback gives thermal energy to the hot halo gas and kinetic energy to the cold halo gas. (x) Mergers bring gas and stars of the satellite galaxy to the bulge of the central galaxy, in major mergers all the mass of the galaxies is given to the bulge of the central galaxy. Bulge radii are computed following Cole et al. (2000). (xi) Disc instabilities bring half of the disc mass into the bulge. (xii) The evolution of the galaxy is followed by numerically integrating a system of equations that follows the dynamics of all the components.

A seed black hole of $1000 M_{\odot}$ is put in the centre of each dark matter halo (see, e.g., Rees 2004 for a discussion on how seed black holes are generated). All the results depend very weakly on the precise mass of the seed black hole, as long as it is not too small.

To be able to accrete onto a black hole, the gas must lose nearly all of its angular momentum. The first loss is connected to the large-scale tidal fields responsible for the formation of a spheroid, due to merger events or disc instabilities. Some low-angular momentum gas can also be available due to the specific distribution of angular momentum within the dark matter halo (Kouschiappas, Bullock & Dekel 2004); in this paper we will not take this possibility into account. The origin of further losses for the cold gas residing in a bulge is unclear. Umemura (2001) proposed that the radiation drag from the UV field of young stars can lead to the creation of a low-angular momentum reservoir of gas, available for accretion onto the black hole. In this case, a fraction $k_{\text{resv}} \sim 10^{-3}$ of the star formation rate can accrete onto the black hole. The interesting point is that many reasonable processes can lead to a linear relation between the creation of the reservoir and the star formation rate (or, equivalently, the amount of cold gas). For instance, turbulence or magnetic fields may be responsible for the loss of angular momentum, and these events are again associated to the formation of massive stars and their consequent explosion as SNe.

If the accretion rate induced by star formation is larger than the Eddington limit, the exceeding gas is put into a reservoir, that is later accreted onto an Eddington time:

$$\dot{M}_{\bullet} = \min \left(k_{\text{resv}} \dot{M}_{\text{sf}} + \frac{M_{\text{resv}}}{t_{\text{ed}}}, \frac{M_{\bullet}}{t_{\text{ed}}} \right), \quad (21)$$

$$\dot{M}_{\text{res}} = k_{\text{resv}} \dot{M}_{\text{sf}} - \dot{M}_{\bullet}. \quad (22)$$

At each merger the black holes are immediately merged as well, and at major mergers the reservoir is destroyed. Granato et al. (2004) have presented a more refined modeling of this reservoir; we prefer however keep a simpler approach here.

The modeling of star formation in bulges is determinant to assess whether quasars are able to trigger galaxy winds. Most semi-analytic codes assume very quick star-formation timescales, of order of the bulge dynamical time. We have shown in Section 3 that following a merger, while it is reasonable that a significant amount of gas is quickly consumed into stars, star-formation timescales will be rather long as soon as self-regulation is achieved. A reasonable compromise is given by forcing the starburst to follow the observational Schmidt law (Schmidt 1959; Kennicutt 1998). The model presented in paper I indeed follows roughly the Schmidt-law, although with a lower normalization (figure 7 of paper I shows that star formation is below the Kennicutt relation if the effective vertical scalelength, here identified with the half-mass radius of the bulge, is of order of 1 kpc). In this case the star-formation timescale is:

$$\tau_{\star} = 2.2 \times 10^8 \frac{M_{\text{cold}}}{10^{11} M_{\odot}} \left(\frac{R_{\text{hm}}}{4.9 \text{ kpc}} \right)^{-2} \text{ yr}. \quad (23)$$

4.2 Low-angular momentum gas and the triggering of the wind

As long as a significant fraction of the stars of a spheroid is formed within the spheroid itself (and not in self-regulated discs that later merge into spheroids), the relation between star formation rate and black hole accretion (equation 21) induces a black hole–bulge correlation similar to that observed for reasonable values of k_{resv} . Many authors (cited in the introduction) have used similar rules in conjunction with hierarchical galaxy formation models, correctly reproducing the black hole–bulge correlation with no need for self-regulation. With our galaxy formation model we find a good fit for the black hole–bulge correlation for $k_{\text{resv}}=0.003$. We demonstrate now that in this case galaxy winds are likely irrelevant.

According to Figure 2, the catastrophic switch from the adiabatic to the PDS confinement regime happens whenever the evaporation rate overtakes the (unperturbed) star-formation rate by a factor of ~ 10 . However, this is valid in the region affected by radiative heating, which for simplicity we assumed in Section 3 to coincide with the whole galaxy; in a realistic case the evaporation is limited to the inner region of the galaxy, $r < R_{\text{rh}}$, which contains only a fraction of the total cold gas and star formation rate (~ 20 per cent in our $10^{11} M_{\odot}$ spheroid case). Even within this region, the evaporation grows linearly with the radius r through the covering factor \mathcal{C} (equation 16), so if the gas distribution in this region is flatter than r^{-2} (and the mass of cold gas grows more rapidly than r) the triggering condition will first be reached in the inner regions and then propagate inside-out⁴. A reasonable and simple triggering criterion for a star-forming galaxy is then obtained when evaporation overtakes

⁴ Besides, the condition of adiabatic confinement requires that

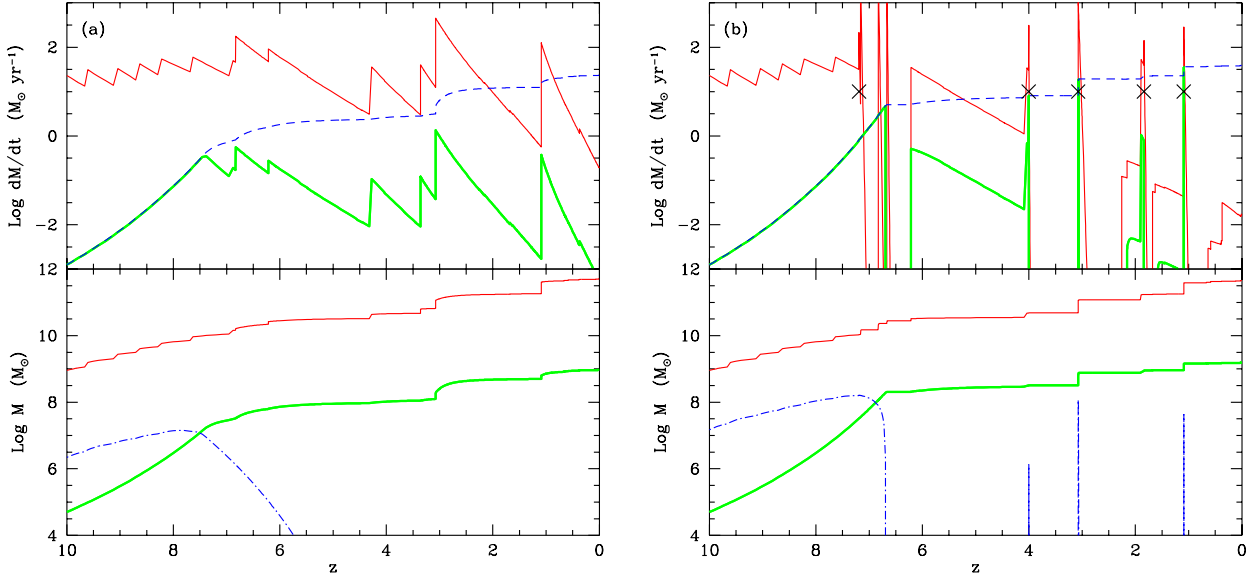


Figure 3. Evolution of the main progenitor of an elliptical galaxy contained in a $1.1 \times 10^{13} M_{\odot}$ dark matter halo. (a): no winds ($k_{\text{resv}}=0.003$). (b): with winds ($k_{\text{rh}}=50$, $k_{\text{resv}}=0.02$ and $k_{\text{trigger}}=1$). Upper panels: star formation rate in the bulge of the main progenitor (continuous lines), accretion rate on the black hole (heavy continuous lines), Eddington limit (dashed lines). The crosses in the right panel denote the shining events. Lower panels: stellar mass of the bulge of the main progenitor (continuous lines), black hole mass (heavy continuous lines), reservoir mass (dot-dashed lines).

the *global* star-formation rate by a factor k_{trigger} of order unity:

$$\dot{M}_{\text{rh}} > k_{\text{trigger}} \dot{M}_{\text{sf}}. \quad (24)$$

Using equations 14, 21 (assuming that accretion is not Eddington limited) and 24, it is easy to see that winds will be triggered if $k_{\text{trigger}} < k_{\text{rh}} \times k_{\text{resv}}$. For $k_{\text{resv}}=0.003$ (the value with which the black hole–bulge correlation is reproduced with no winds) and $k_{\text{rh}}=50$, this implies $k_{\text{trigger}} < 0.15$. In other words, winds will work only if radiative heating is concentrated on ~ 1.5 per cent of the star-forming region. The result of switching winds in this case is to limit black hole masses to lower values, with a resulting underestimate.

Alternatively, the mass deposition rate on the reservoir can be higher. In this case the black hole–bulge correlation is due to the self-limiting action of winds. Keeping $k_{\text{rh}}=50$ and assuming $k_{\text{trigger}}=1$, winds are triggered if $k_{\text{resv}} \geq 0.02$, nearly an order of magnitude higher than before.

To be more specific, a massive wind in the galaxy formation model is triggered whenever: (i) the triggering condition of equation 24 is satisfied; (ii) the accretion rate in Eddington units is larger than 0.01 (otherwise the system switches to a radiatively inefficient accretion mode, and the present model does not apply); (iii) the amount of cold mass present in the bulge is lower than equation 20. To implement the post-wind scenario described in Section 3, 10 per cent of the cold gas is not put into the shell but consumed by star formation on a bulge dynamical time, while a fraction k_{resv} of this gas is put in the reservoir to be accreted onto

the gas distribution is flatter than r^{-2} up to the vertical scale-length of the system.

the black hole. The cold gas in the shell is then given to the cold halo component.

The main uncertainties and degrees of freedom in the modeling of the wind are the following: (i) the timescale of star formation in bulges is fixed in a phenomenological way, better modeling is needed. (ii) The modeling of the reservoir of low-angular momentum gas is reasonable but not unique. (iii) The parameter k_{rh} is fixed with no explicit reference to R_{rh} or to the covering factor of cold clouds. (iv) The parameter k_{resv} is very poorly constrained. (v) The constant in equation 20 depends on many uncertain details and may reasonably be considered as a free parameter (we will keep it fixed to the value given above). (vi) The parameter k_{trigger} is uncertain by at least a factor of ten. (vii) The fraction of mass compressed to the centre after the wind is uncertain as well.

4.3 An example

In this subsection we show that there is a significant part of the parameter space that allows for quasar-triggered galaxy winds, and briefly outline the effect these would have on the galaxy population as a whole.

We have taken a $1.1 \times 10^{13} M_{\odot}$ dark matter halo from a 256^3 PINOCCHIO realization of size 93 Mpc. The particle mass for this box is 3×10^9 , corresponding to a mass resolution for the merger tree of $\sim 10^{11} M_{\odot}$. Due to its particular merger history, this halo hosts a spheroid at the final time ($z = 0$). The mass of the spheroid depends of course on the details of galaxy formation, and ranges from 10^{11} to $5 \times 10^{11} M_{\odot}$. We have run the model assuming first no winds ($k_{\text{rh}}=0$), so that the black hole–bulge correlation is set by angular momentum loss ($k_{\text{resv}}=0.003$). Figure 3a shows the resulting

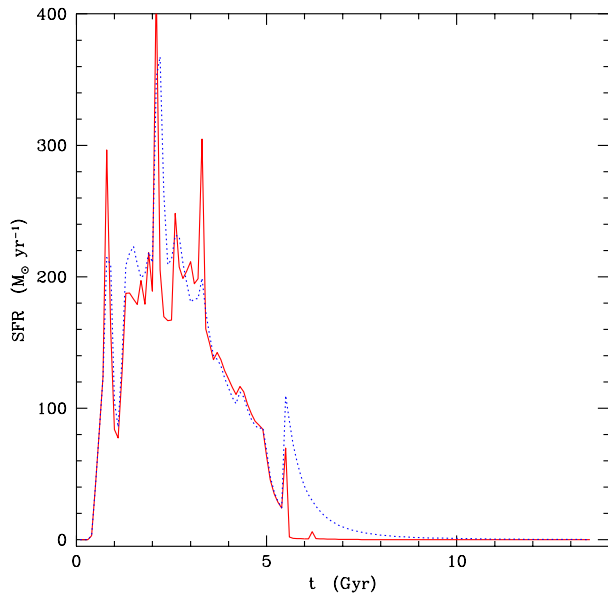


Figure 4. Star formation rates for the two examples shown in Figure 3. This time the star formation rate of all the stars contained in the galaxy at $z = 0$ is given. The dotted line refers to the example without winds (Figure 3a), the continuous line to the example with winds (Figure 3b).

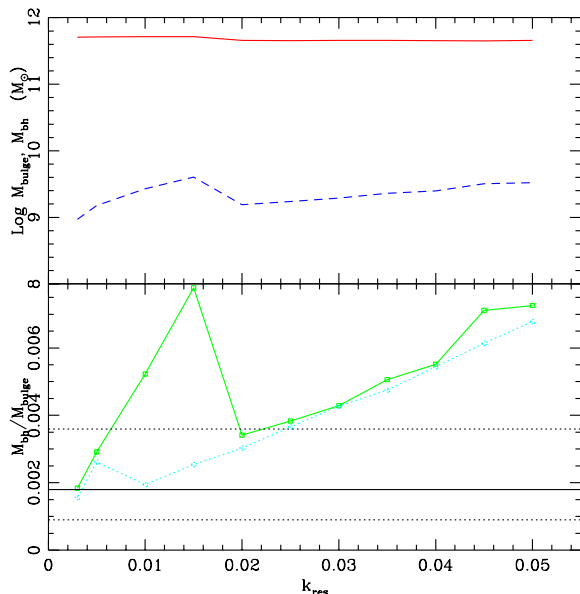


Figure 5. Upper panel: bulge (continuous line) and black hole (dashed line) masses as a function of k_{resv} for the example of Figure 3 ($k_{\text{trigger}}=1$). Lower panel: black hole–bulge ratio as a function of k_{resv} for the case $k_{\text{trigger}}=1$ (continuous line) and $k_{\text{trigger}}=0.3$ (dotted line). The horizontal continuous and dashed lines show the range allowed by observations (Shankar et al. 2004).

evolution of the main progenitor of the galaxy. In particular, we show accretion and star formation rates, bulge, black hole and reservoir masses. It is worth clarifying that all these quantities refer to the bulge of the main progenitor; accretion takes place also in the black holes of satellite galaxies, while stars form both in satellites and discs.

In this case of no wind, the assembly of the galaxy proceeds gradually. The two main star-formation events are located at $z \sim 3$ and ~ 1 , while the sawtooth-like events at very high redshift are due to successive disc instabilities. The black hole starts accreting mass at very early times, and its accretion is Eddington limited till $z \sim 7.5$. By $z \sim 6$ a $\sim 10^8 M_{\odot}$ black hole is already present. The two main shining events closely follow the mergers, and are both sub-Eddington. Most black hole mass is acquired by accretion more than by black hole mergers. At the final time the bulge and black hole masses are 5.1×10^{11} and $9.4 \times 10^8 M_{\odot}$, compatible with the observational black hole–bulge relation.

Figure 3b shows the same example with $k_{\text{rh}}=50$ and $k_{\text{resv}}=0.02$. The evolution at very high redshift is similar, but the Eddington accreting phase goes on for a longer time (due to the higher amount of low-angular momentum gas available), so that the resulting black hole is a factor of 3 more massive at redshift ~ 6 . The first shining event takes place at $z \sim 7$, and has the effect of quenching star formation in the spheroid. Further shinings take place at redshifts ~ 4 , 3, 2 and 1. In each case we have a short quasar phase that however contributes significantly at the mass of the black hole only at redshift 3 (with a significant burst at $z \sim 1$). In the meantime, the episodes of star formation are quickly quenched. As a result, the final bulge and black hole masses are 4.6×10^{11} and $1.6 \times 10^9 M_{\odot}$. This galaxy lies a factor of 2 above the observational relation, just below the $1\text{-}\sigma$ 0.3 dex dispersion.

Figure 4 shows, as a function of cosmological time, the star formation rates of all the stars contained in the final spheroid for the two cases. This is different from the star formation rate of the bulge of the main progenitor, as it contains the contribution of stars formed in discs and satellites. The two star formation rates do not differ much; the most notable effect is the truncation of the low-redshift tail of star formation. This detail however can be very important because minor episodes of star formation can influence strongly the luminosity-weighted colours of galaxies. Moreover, the chemical evolution of these object is also affected by late star formation events, that take place from iron-enriched material and decrease the α -enhancement (see, e.g., Matteucci 1996). The effect of winds will then be to increase the number of passive old galaxies at $z \sim 1\text{--}2$ and to allow a high level of α -enhancement.

Besides, the quasar population will be more deeply affected by winds, especially for $M_{\text{bul}} < 10^{10} M_{\odot}$, where SNe alone are able to generate a massive wind. In this case we expect an increase of bright quasars at very high redshift (because the Eddington limited phase lasts longer) and a decrease at low redshift (because the shining events are suppressed by winds), in agreement with the trends suggested by observations.

Figure 5 shows how the black hole and bulge masses and their ratio change when the k_{resv} parameter is increased; for $k_{\text{resv}} < 0.02$ both black hole mass and ratio grow linearly with k_{resv} , but as soon as winds come into play the frac-

tion self-regulates to a value that remains relatively stable till $k_{\text{resv}}=0.03$, then starts growing again. The upper panel shows that the main effect of wind triggering is on the black hole, though bulges tend to be slightly less massive. Finally, a good value for the black hole–bulge ratio is obtained with $k_{\text{trigger}}=0.3$ and $k_{\text{resv}}=0.01$ (dotted line)

5 CONCLUSIONS

Radiation pressure and radiative heating are two unavoidable processes during the shining of a quasar that strongly influence the ISM of a star-forming spheroid. However, taken alone they may not be able to trigger those massive winds that have often been assumed to take place during the formation of a spheroidal galaxy. Based on a model for feedback in galaxy formation, we have proposed that a massive removal of ISM from a large star-forming spheroid can be triggered by the joint action of SNe and quasar light as follows: (i) stars form in a self-regulated way in a two-phase, highly pressurized ISM; (ii) through runaway radiative heating, the quasar evaporates part of the cold phase; (iii) when the evaporation rate is strong enough, the feedback regime changes: due to the higher density of the hot phase, SBs arising from the star-forming clouds get to the PDS stage before being halted by pressure confinement; (iv) the consequent drop in pressure leads to the percolation of cold shells and to the creation of an expanding super-shell; (v) some mass is compressed to the centre, giving rise to a nuclear starburst and to further black hole accretion; (vi) the remaining cold gas (not included in the shell or in the nucleus) is most likely involved in diffuse star formation; (vii) radiation pressure pushes the shell out of the galaxy if it is not too massive; (viii) as soon as it interacts with the external hot halo gas, the shell halts and fragments; (ix) a part of it is finally evaporated by radiative heating, though to a much lower temperature than the inverse Compton one of the quasar.

We have demonstrated that this mechanism can lead to a self-limited black hole–bulge relation similar to the observed one. However, using a galaxy formation model (presently under development) that takes into account black hole accretion, we have shown that the black hole–bulge relation is also reproduced assuming that the rate of deposition of low-angular momentum gas onto the black hole amounts 0.3 per cent of the star formation rate in the bulge. Including a motivated criterion for quasar-triggered winds, we have shown that the black hole–bulge relation is self-limited by winds whenever the deposition rate is at least ~ 1 per cent of the bulge star-formation rate. Compared to the no-wind case, this mechanism leads to more massive black holes at high redshift and to a quenching of low-redshift activity.

There are two main possible objections to this scenario. First, a massive removal of ISM can be caused by other mechanisms, like a kinetic ejection of matter from the AGN (Granato et al. 2004) or simply by radiative heating (Sazonov et al. 2004a) or radiation pressure (Murray et al. 2005) by the quasar light, so there is no real need for such a sophisticated and indirect mechanism. Ejection of matter at nearly relativistic speed is observed in action in extreme BAL quasars; however, this mechanism can work only if the covering angle of the outflow is large. On the other hand, the

radiation of the quasar alone may be able to remove only a modest fraction of the mass of the ISM, not larger than a few per cent. The triggering mechanism suggested here has the merit of creating an outwardly expanding, optically thick super-shell (with unity covering factor), which is then easily pushed away by radiation pressure. An appreciable element is that the prediction comes out naturally from the model of paper I without any parameter tuning.

The second objection is that if a reservoir of low angular momentum gas is created at a rate proportional to the star-formation rate in bulges, then there is no need for a self-limiting mechanism responsible for the black hole–bulge relation. In this case the condition for wind triggering may never (or almost never) be reached in practice. Probably the strongest argument in favour of winds lies in the chemical enrichment patterns of bulges (stars, ISM and circum-quasar gas), but more work is needed for an assessment of this point.

It is not easy to devise critical observational tests to understand if a mechanism like the one described here is actual. Due to the number of processes involved and to the huge uncertainties in many of the parameters, many different configurations may lead to very similar predictions. To be more specific, all the evolution from the starburst to the ejection of the shell would be hidden by dust, so the quasar would be invisible. Shining quasars would correspond to the stage after the destruction of the shell, so the only clearly observable stage would correspond to the last phases of expulsion and evaporation of the shell. For $k_{\text{th}}=50$ this takes a time $t \sim 5 \times 10^8 f_s M_{\text{bul},11} \dot{M}_{\bullet,4}$ yr, so a massive shell would be visible for $\sim 12 \times f_s$ Eddington times as an absorber with a low expansion velocity. Such objects are seen for instance in absorption of optical quasar spectra (see, e.g., Srianand & Petitjean 2000; D’odorico et al. 2004). Their structure is generally very complex, and outflowing speeds range from hundreds to tens of thousands of km s^{-1} . A quick and dirty comparison with such data is then impossible, and more precise predictions need a dedicated calculation and will be presented elsewhere.

Another way to probe the validity of the wind model is through its effects on the statistical properties of galaxies. In this case the problem is in the degeneracy with all the other (numerous and uncertain) parameters of galaxy formation. Anyway, the higher accretion rate connected with quasar triggered winds gives more massive black holes at $z \sim 6$ and a quenching of low- z activity, in line with the observational evidence, while the expulsion of the metals generated after the first burst of star formation is in line both with the high level of alpha enhancement of ellipticals and with the high abundance of iron in clusters. Moreover, the fact that no limit on the fraction of mass that can be removed is present for bulges less massive than $10^{10} M_{\odot}$ implies an increase in the scatter of the black hole–bulge relation at small masses; the observations for such small bulges are few, but the possible finding of outliers in the relation would be in line with this prediction. A more accurate analysis will be presented in a subsequent paper.

ACKNOWLEDGMENTS

We thank Giuliano Taffoni for his help in developing the galaxy formation code, and Stefano Cristiani, Mitch Begelman and Gianluigi Granato for discussions.

REFERENCES

- Begelman M.C., 1985, *ApJ*, 297, 492
 Begelman M.C., 2004, in L.C. Ho ed., *Coevolution of Black Holes and Galaxies*. Cambridge University Press, Cambridge, p. 375
 Begelman M.C., McKee C.F., Shields G.A., 1983, *ApJ*, 271, 70
 Bromley J.M., Somerville R.S., Fabian A.C., 2004, *MNRAS*, 350, 456
 Cattaneo A., 2001, *MNRAS*, 324, 128
 Cavaliere A., Vittorini V., 2002, *ApJ*, 570, 114
 Cioffi, D.F., McKee, C.F., Bertschinger, E., 1988, *ApJ*, 334, 252
 Ciotti L., Ostriker J.P., 1997, *ApJ*, 487, L105
 Cole S., Lacey C.G., Baugh C.M., Frenk C.S., 2000, *MNRAS*, 319, 168
 Comastri A., Setti G., Zamorani G., Hasinger G., 1995, *A&A*, 296, 1
 Cristiani S., Vio R., 1990, *A&A*, 227, 385
 D'odorico V., Cristiani S., Romano D., Granato G.L., Danese L., 2004, *MNRAS*, 351, 976
 Dunlop J.S., McLure R.J., Kukula M.J., Baum S.A., O'Dea C.P., Hughes D.H., 2003, *MNRAS*, 340, 1095
 Edge A.C., Frayer D.T., 2003, *ApJ*, 594, L13
 Elmegreen B.G., 2002, *ApJ*, 564, 773
 Fabian A.C., 1999, *MNRAS*, 308, 39
 Granato G.L., De Zotti G., Silva L., Bressan A., Danese L., 2004, *ApJ*, 600, 580
 Granato G.L., Silva L., Monaco P., Panuzzo P., Salucci P., De Zotti G., Danese L., 2001, *MNRAS*, 324, 757
 Haehnelt M.G., Natarajan P., Rees M.J., 1998, *MNRAS*, 300, 817
 Haiman Z., Ciotti L., Ostriker J.P., 2004, *ApJ*, 606, 763
 Hamann F., Ferland G., 1999, *ARA&A*, 37, 487
 Häring N., Rix H.W., 2004, *ApJ*, 604, 89
 Hatton S., Devriendt J.E.G., Ninin S., Bouchet F.R., Guiderdoni B., Vibert D., 2003, *MNRAS*, 343, 75
 Hatziminaoglou E., Mathez G., Solanes J., Manrique A., Salvador-Solé E., 2003, *MNRAS*, 343, 692
 Kang X., Jing Y.P., Mo H.J., Boerner G., 2004, *astro-ph/0408475*
 Kauffmann G., Haehnelt M.G., 2000, *MNRAS*, 311, 576
 Kauffmann G., Colberg J.M., Diaferio A., White S.D.M., 1999, *MNRAS*, 307, 529
 Kennicutt R.C., 1998, *ApJ*, 498, 541
 Kormendy J., Richstone D., 1995, *ARA&A*, 33, 581
 Koushiappas S.M., Bullock J.S., Dekel A., 2004, *MNRAS*, 349
 Kriss G.A., Davidsen A., Zheng W., Lee G., 1999, *ApJ*, 527, 683
 Krolik J.H., McKee C.F., Tarter C.B., 1981, *ApJ*, 249, 422
 Lombardi M., Bertin G., 2001, *A&A*, 375, 1091
 Magorrian J., Tremaine S., Richstone D. et al., 1998, *ApJ*, 115, 2285
 Mahmood A., Devriendt J.E.G., Silk J., *astro-ph/0401003*
 Maiolino R., Oliva E., Ghinassi F., Pedani M., Mannucci F., Mujica R., Juarez Y., 2004, *A&A*, 420, 889
 Marconi A., Hunt L.K., 2003, *ApJ*, 589, 21
 Matteucci F., 1994, *A&A*, 288, 57
 Matteucci F., 1996, *Fund. Cosm. Phys.*, 17, 283
 Matteucci F., Padovani P., 1993, *ApJ*, 419, 485
 Menci N., Cavaliere A., Fontana A., Giallongo E., Poli F., Vittorini V., 2003, *ApJ*, 587, 63
 Mo H.J., Mao S., White S.D.M., 1998, *MNRAS*, 295, 319
 Monaco P., Theuns T., Taffoni G., Governato F., Quinn T., Stadel J., 2002, *ApJ*, 564, 8
 Monaco P., Theuns T., Taffoni G., 2002, *MNRAS*, 331, 587
 Monaco P., 2004a, *MNRAS*, 352, 181 (paper I)
 Monaco P., 2004b, *MNRAS*, 354, 151
 Monaco P., 2004c, in eds. A. Merloni, S. Nayakshin, R. Sunyaev, *Growing Black Holes*. Springer-Verlag, Berlin, in press
 Mori M., Ferrara A., Madau P., 2002, *ApJ*, 571, 40
 Murray N., Quataert E., Thompson T.A., 2005, *ApJ*, 618, 569
 Ostriker J.P., McKee C.F., 1988, *RvMP*, 60, 10
 Ostriker J.P., Ciotti L., 2004 (*astro-ph/0407234*)
 Rees M., 2004, in eds. A. Merloni, S. Nayakshin, R. Sunyaev, *Growing Black Holes*. Springer-Verlag, Berlin, in press
 Renzini A., 2004, in eds. J.S. Mulchaey, A. Dressler, A. Oemler 2004, *Clusters of Galaxies: Probes of Cosmological Structure and Galaxy Evolution*. Carnegie Observatories Astrophysics Series. Pag 261
 Risaliti G., Elvis M., 2004, (*astro-ph/0403361*)
 Romano D., Silva L., Matteucci F., Danese L., 2002, *MNRAS*, 334, 444
 Salucci P., Szuszkiewicz E., Monaco P., Danese L., 1999, *MNRAS*, 307, 637
 Sazonov S.Yu., Ostriker J.P., Ciotti L., Sunyaev R.A., 2004a, submitted to *MNRAS* (*astro-ph/0411086*)
 Sazonov S.Yu., Ostriker J.P., Sunyaev R.A., 2004b, *MNRAS*, 347, 144
 Schmidt M., 1959, *ApJ*, 129, 243
 Silk J., Rees M.J., 1998, *A&A*, 331, 1
 Shankar F., Salucci P., Granato G.L., De Zotti G., Danese L., 2004, *MNRAS*, 354, 1020
 Somerville R.S., Primack J.R., Faber S.M., 2001, *MNRAS*, 320, 504
 Springel V., Di Matteo T., Hernquist L., 2004, submitted to *MNRAS* (*astro-ph/0411108*)
 Srianand R., Petitjean P., 2000, *A&A*, 357, 414
 Sutherland R.S., Dopita M.A., 1993, *ApJS*, 88, 253
 Taffoni G., Mayer L., Colpi M., Governato F., 2003, *MNRAS*, 341, 434
 Taffoni G., Monaco P., Theuns T., 2002, *MNRAS*, 333, 623
 Thomas D., 1999, *MNRAS*, 306, 655
 Umemura M., 2001, *ApJ*, 560, 29
 Vignali C., Brandt W.N., Schneider D.P., 2003, *ApJ*, 125, 433
 Yu Q., Tremaine S., 2002, *MNRAS*, 335, 965
 Weaver R., McCray R., Castor J., Shapiro P., Moore R., 1977, *ApJ*, 218, 377

This paper has been typeset from a \TeX / \LaTeX file prepared by the author.